P and S wave separation at a liquid-solid interface

Maria S. Donati and Robert R. Stewart

ABSTRACT

P and S seismic waves impinging on a liquid-solid interface give rise to energy on both horizontal and vertical geophones. The response of the vertical geophone at an interface is quite similar to that on a free surface. The horizontal geophone has a stronger response to impinging P waves and a smoother response to incident S waves. Presented here is a filtering method operating in the τ-p domain, that separates P and S waves by taking into account the geophone response. The filter requires estimates of the near-interface P and S wave velocities but is robust with respect to errors in these velocities. The P-S separation filter is tested on synthetic elastic-wave data and performs the wave type separation well.

INTRODUCTION

The quest for a more detailed and confident description of the subsurface has led to the rise of three-component (3-C) seismic surveying. Considerable effort is currently being expended to make and use converted-wave (P-to-S reflection) seismic sections from these 3-C recordings. Most of the effort to date has been with land recordings. However, with the advent of the SUMIC (subsea seismic) survey and its very promising early results (Berg et al., 1994; Granli et al., 1995), more attention is focusing on the marine 3-C case (Fig. 1). A fundamental aspect of deciphering 3-C records from the ocean bottom is to understand how seismic waves interact with a geophone at a fluid-solid interface. This paper reviews the basic theory of the geophone response at the water bottom and proposes a new filter to separate P and S waves so recorded. The separation filter is based on the methods of Dankbaar (1985) and Labonte (1990). The separated waves (pure P and S) are then further processed into their respective sections.

THEORY

The P-S separation method here uses the water-bottom geophone response as developed by White (1965). The geophone response describes the P and S amplitudes output from a receiver due to an incident wave of "unit" size. This output varies with the angle of incidence of the impinging waves. In the elastic case considered here, four responses are involved, distinct for vertical and horizontal geophones and for incident P and S waves.

The expressions for the response of a single geophone located at a liquid-solid contact (White, 1965) can be written as a function of horizontal slowness p, which is defined as the reciprocal of velocity along the horizontal direction ($p= \sin\theta/V$, θ is the

incidence angle measured from the vertical). The vertical geophone response $R_V^P(p)$ from an impinging P wave, at angle ϕ, with horizontal slowness p is given below, where primed quantities are related to the liquid:

$$R_V^P(p) = 2\gamma^{-1}\xi * (2V_s^2 p^2 - 1)\big/ R_o(p), \tag{1}$$

where $\gamma = V_s\big/V_p$, $\xi = (\gamma^2 - V_s^2 p^2)^{1/2}$, and

$$R_o(p) = \frac{\rho' V_p'(1-V_p^2 p^2)^{1/2}}{\rho V_p(1-V_p'^2 p^2)^{1/2}} + 4\gamma^3 \sin^2\phi \cos\phi (1-\gamma^2 \sin^2\phi)^{1/2} + (1-2\gamma^2 \sin^2\phi)$$

The response from an impinging S wave is:

$$R_V^S(p) = 4V_s p\eta\xi \big/ R_o(p), \tag{2}$$

where $\eta = (1 - V_s^2 p^2)^{1/2}$.

Similarly the horizontal geophone response from an impinging P wave is:

$$R_H^P(p) = 2V_p p * \left[\frac{\rho' V_p'(1-V_p^2 p^2)^{1/2}}{\rho V_p(1-V_p'^2 p^2)^{1/2}} + 2\xi\eta\right]\bigg/ R_o(p), \tag{3}$$

and the horizontal geophone response from S wave is:

$$R_H^S(p) = 2\eta * \left[\frac{\rho' V_p'(1-V_p^2 p^2)^{1/2}}{\rho V_p(1-V_p'^2 p^2)^{1/2}} + (1-2V_s^2 p^2)\right]\bigg/ R_o(p), \tag{4}$$

To view the geophone responses, let us take a specific case where the solid has elastic values: ρ= 1.6 g/cc, Vp= 1500 m/s, and Vs= 650 m/s, and the fluid has values: ρ= 1.135 g/cc and Vp= 1455 m/s. The geophone responses are shown as functions of angle of incidence in Fig. 2. We can compare these responses with those from a geophone on a free surface. Using the same solid values and the expressions of the response on a free surface (White, 1965), we calculated the plots in Fig. 3. Figs. 2a and 3a show the behavior of the vertical geophone for a stress-free solid and liquid-solid contact, respectively. We see that the magnitudes of the geophone responses at a liquid-solid contact are reduced as compared with the stress-free solid. The S-wave response in the fluid case is also relatively smaller compared to the P-wave.

The horizontal geophone responses for a stress-free solid and liquid-solid contact are plotted in Figs. 2b and 3b. We see that R_H^S is modified somewhat by the presence of the liquid: the principal effects being the elimination of the nulls at 45°, and the increased sensitivity to the incident P waves.

To derive the P-S separation filter, we first express the full horizontal and vertical geophone records in terms of the response to incident P and S waves. As shown before, these responses are a function of horizontal slowness, thus it is advantageous to decompose the data into plane waves, i.e. to transform the data to the τ-p domain. Then the expressions become straightforward:

$$U_V(\tau, p) = P_{in}(\tau, p)R_V^P(\tau, p) + S_{in}(\tau, p)R_V^S(\tau, p), \tag{5}$$

$$U_H(\tau, p) = P_{in}(\tau, p)R_H^P(\tau, p) + S_{in}(\tau, p)R_H^S(\tau, p), \tag{6}$$

where U_V and U_H are the vertical and horizontal geophone records transformed to the τ-p domain, P_{in} and S_{in} the incident P and S wavefields, and R_V^P, R_V^S, R_H^P and R_H^S the geophone responses, respectively.

If we have records from both horizontal and vertical geophones (U_H and U_V), then we have two equations with two unknowns (the incident P and incident S waves). The equations can be solved for P and S waves:

$$P_{in}(\tau, p) = F_V^P(\tau, p)U_V(\tau, p) + F_H^P(\tau, p)U_H(\tau, p), \tag{7}$$

$$S_{in}(\tau, p) = F_V^S(\tau, p)U_V(\tau, p) + F_H^S(\tau, p)U_H(\tau, p), \tag{8}$$

The coefficients F are functions of geophone responses R and are considered as filter coefficients. The subscripts V or H indicate that the coefficients operate on vertical or horizontal geophone data, superscript P or S, respectively, indicates coefficients for the pass-P or pass-S mode. The full expressions for the F functions are given below:

$$F_V^P = \frac{-R_H^S}{R_H^P R_V^S - R_V^P R_H^S} = \frac{-\gamma(m_o + (1 - 2V_s^2 p^2))}{2\xi} \tag{9}$$

$$F_H^P = \frac{R_V^S}{R_H^P R_V^S - R_V^P R_H^S} = \gamma^2 V_p p \tag{10}$$

$$F_V^S = \frac{-R_H^P}{R_H^S R_V^P - R_V^S R_H^P} = \frac{V_s p(m_o + 2\xi\eta)}{2\xi\eta} \tag{11}$$

$$F_H^S = \frac{R_V^P}{R_H^S R_V^P - R_V^S R_H^P} = \frac{(1 - 2V_s^2 p^2)}{2\eta} \tag{12}$$

where $m_o = \rho V_p' (1 - V_p^2 p^2)^{1/2} \Big/ \rho V_p (1 - V_p'^2 p^2)^{1/2}$.

The geophone responses and thus the filter coefficients are only functions of p and the fluid and solid elastic parameters.

Fig. 4a shows the four filter coefficients as functions of slowness for the elastic parameters as in Figs. 2 and 3. The maximum slowness displayed corresponds to that of incident S waves. These results can be compared with the four filter coefficients of the P-S separation filter related to stress-free solid (Fig. 4b). The filter coefficients have similar shapes except for F_V^S which shows a non-linear behavior with the horizontal slowness p due to the additional term $V_S p m_o / 2\xi\eta$, and becomes large at the maximum slowness of the incident P waves. Also, the coefficients F_V^S and F_V^P for the fluid-solid interface are affected by the variable m_o which contains information on the elastic properties of both media. In both cases, the F_H^P and F_V^P filter coefficients are limited by the maximal slowness of the incident P waves which represents horizontal incidence. The values of the filter coefficients for the liquid-solid contact have been limited to avoid instabilities in the P-S separation filter similar to what is done in the stress-free interface case (Labonté, 1990) (Fig. 4a,b).

The filter is operated in pass-P or pass-S mode. In pass-P mode, the output consists of all waves arriving at the liquid-solid contact as P waves: S wave energy is removed. In pass-S mode, the output is the incident S wavefield, with P wave energy removed. To return to the x-t domain, an inverse τ-p transform is applied.

Fig. 5 shows the basic steps followed by the P-S separation filter in the τ-p domain. The procedure followed for calculating the direct and inverse τ-p transformation is similar to Stoffa et al. (1981).

TESTING

Some examples of the filter operation on synthetic data follow. A horizontally layered earth model (after Dankbaar, 1985) is used and shown in Fig. 6. There are six flat homogeneous layers on top of a half-space. The first layer consists of a water layer

10 m deep and the maximum reflector depth in this model is 210 m. Geophone offsets are from 5-140 m, spaced every 5 m. The synthetic data are calculated using the Uniseis (Landmark Graphics Corp.) seismic modeling package which employs ray tracing and spherical spreading.

First, we consider the source located at the top of the water layer and the receivers on the bottom of the water layer and the top of layer 2 (solid). In this case, the explosive source (*P* waves only) radiated energy uniformly from 0° to 180° downward. Only *P-P* and *P-S* primary reflections are considered. Fig. 7a shows the *P-P* and *P-S* seismograms without geophone responses, where only *P* wave arrivals for the vertical geophone and only *S* wave arrivals for the horizontal geophone are considered. In other words, each geophone is considered having receiving characteristics patterns without mode-interference. The *P-P* and *P-S* seismograms were generated using a minimum phase wavelet with a center frequency of 50 Hz. Then, the *P-P* seismogram represents the response of the vertical geophone taking R_V^S equal zero; likewise with the *P-S* seismogram with R_H^P equal zero. Next, taking into account the geophone responses and using (Fig. 2) incident *P* and converted waves gives traces as shown in the Figs. 7b. On the horizontal geophone record all *P-P* and *P-S* reflections are evident.

The filtered pass-*P* and pass-*S* are shown in Fig. 7c. They can be compared with the incident seismograms (Fig. 7a). There is reasonable agreement between the corresponding records indicating fairly good wave-type separation.

The effect on the filter of erroneous estimates of the layer 2 velocities is shown in Fig. 8. The vertical and horizontal geophone records from Fig. 7b were filtered using erroneous values as follows: first we use Vp= 1600 m/s and Vs= 750 m/s for layer 2 (which represent a 10% error), and density ρ= 1.6 g/cc for the solid, and Vp= 1455 m/s and ρ= 1.135 g/cc for the liquid. The filtered sections are shown in Fig. 8a. Next 20% errors are used in the layer 2 velocities giving Vp= 1700 m/s and Vs= 850 m/s, and density ρ= 1.6 g/cc for the solid, and Vp= 1455 m/s and ρ= 1.135 g/cc for the liquid. The resultant sections are shown in Fig. 8b. Finally, perturbed parameters in velocity and density are used Vp= 1600 m/s and Vs= 800 m/s and density ρ= 1.3 g/cc for the solid, and Vp= 1350 m/s and ρ= 1.0 g/cc for the liquid. The filtered sections are shown in Fig. 8c.

The results presented in Figs. 8a,c can be compared with the records from Fig. 7a. The similar results of the filter when using erroneous velocities and densities for the calculation indicate a robust operation. We see that the pass-*P* record is less effected by errors in the velocities than the pass-*S* record, where there is still some residual *P*-wave energy.

In the second case, we consider both the source and the receivers located on the liquid-solid contact. First, only *P-P* and *S-S* reflections were calculated, where both *P*

and S waves were radiated by the source. Fig. 9a shows the incident P and S waves at the liquid-solid contact with no geophone responses. The incident S waves have zero points at certain offsets, followed by a nearly 180° phase shift for larger offsets. The vertical and horizontal geophone records are shown in the Fig. 9b. All P and S arrivals appear on both records. The shallow SS-2 reflection interferes with the PP-4 and PP-5 reflections and P reflections complicate the horizontal response.

The result of the separation filter applied on both vertical and horizontal records is shown in the Fig. 9c. The filter used near-surface velocities Vp= 1500 m/s and Vs= 650 m/s, and density ρ=1.6 g/cc for the solid and velocity Vp= 1455 m/s and density ρ= 1.135 g/cc for the liquid, as corresponds to the velocities for the liquid and first solid layer in the synthetic model.

The comparison of the filtered pass-P and pass-S records with the incident seismograms shows a reasonable performance. Most of the S-wave energy is removed from the pass-P section. However, there is some P wave leakage onto the pass-S section. This is largely due to errors of the τ-p transform and some instabilities in the filter coefficients. Some noise is present on both pass-P and pass-S records as consequence of the limitations during the summation process in the τ-p domain.

The same experiment performed in Figs. 8a,c (with erroneous layer 2 values) is now applied on the horizontal and vertical geophone records shown in Fig. 9b. Figs. 10a,c display the filtering effects when erroneous velocities Vp and Vs are used. Once again, the filter is robust with respect to errors in the velocity estimates.

The last example presents a more complex situation in separating P and S waves. Again both source and receivers are located at the bottom of the water layer, but converted P-S and S-P reflections are included. Fig. 11a shows the incident P-P and S-P and incident S-S and P-S waves. The S-P converted reflections have quite low amplitudes in comparison with the converted P-S waves. Fig. 11b shows the vertical and horizontal geophone records resulting from the incident P and S waves. The resultant pass-P and pass-S (Fig. 11c) can be compared with the incident seismograms (Fig. 11a). There is good agreement between the corresponding records. The incident P and S waves are retrieved correctly, although SS-2 and SS-3 have slightly lower amplitudes after the filtering process.

Figs. 12a,c shows the results of testing the stability of the filter against errors in the P and S velocity. These results can be compared with the incident P and S waves in Fig. 11a. We see that the separation of P and S waves is still successful. The PP-2 reflection is somewhat larger than when filtering with the correct velocity specified.

CONCLUSIONS

This paper reviews the response of a two-component geophone at a fluid-solid interface and presents a filtering method to separate incident P and S waves. We find that there are some differences between the responses of a geophone located on a

stress-free solid and geophone located at a liquid-solid contact. The response of the vertical channels are reduced in the liquid-solid case compared to the free surface. There is also a smoother response for shear waves on the horizontal channel in the fluid-solid case.

A *P-S* separation filter is developed which uses the geophone responses and operates in the τ-p domain. It performs well on synthetic data when the source is located on the top of the water layer and the receivers located at the bottom of the water layer. It also provides good results for data recorded with both source and receivers located on the bottom of the water layer. The filter is stable with respect to errors in the elastic values of layer under the fluid. Because of the *S*-wave energy on the vertical channel and *P*-wave energy on the horizontal channel, it will be very useful to separate wave types before proceeding on to make pure *P* and *S* wave section.

ACKNOWLEDGMENTS

REFERENCES

Berg, E., Svenning, B., and Martin, J., 1994, SUMIC: Multicomponent sea-bottom seismic surveying in the North Sea-Data interpretation and applications: Presented at the 64th Ann. Internat. Mtg., Soc. Expl. Geophys., Expanded Abstracts, 477-480.

Dankbaar, J.W.M., 1985, Separation of P- and S-waves: Geophys. Prosp., 33, 970-986.

Ferber, R.G., 1989, On the design of 2-D convolution filters for separation of *P*- and *S*-waves: Presented at the 59th Ann. Internat. Mtg., Soc. Expl. Geophys., Expanded Abstracts, 1101-1103.

Granli, J.R., Sollid, A., Hilde, E., and Arnsten, B., 1995, Imaging through gas-filled sediments with marine *S*-wave data: Presented at the 65th Ann. Internat. Mtg., Soc. Expl. Geophys., Expanded Abstracts, 352-355.

Labonté, S., 1990, Modal separation, mapping, and inverting three-component VSP data M. Sc. Thesis, The University of Calgary, Calgary.

Stoffa, P.L., Buhl, P., Diebold, J.B., and Wenzel, F., 1981, Direct mapping of seismic data to the domain of intercept time and ray parameter-a plane wave decomposition: Geophysics, 46, 255-267.

White, J.E., 1965, Seismic waves radiation, transmission and attenuation: McGraw-Hill, Inc.
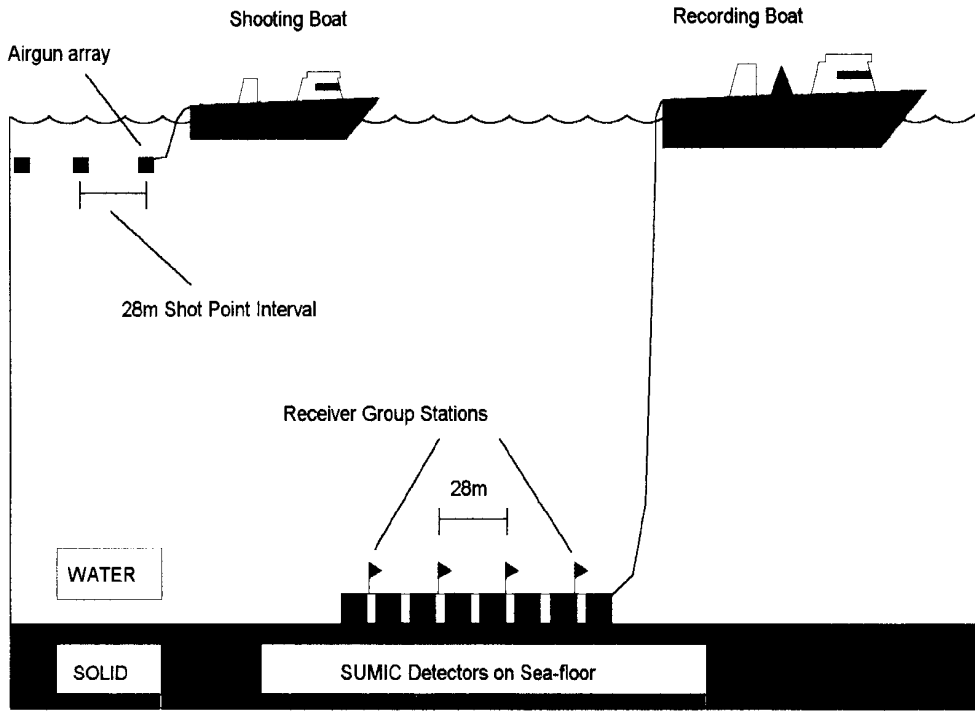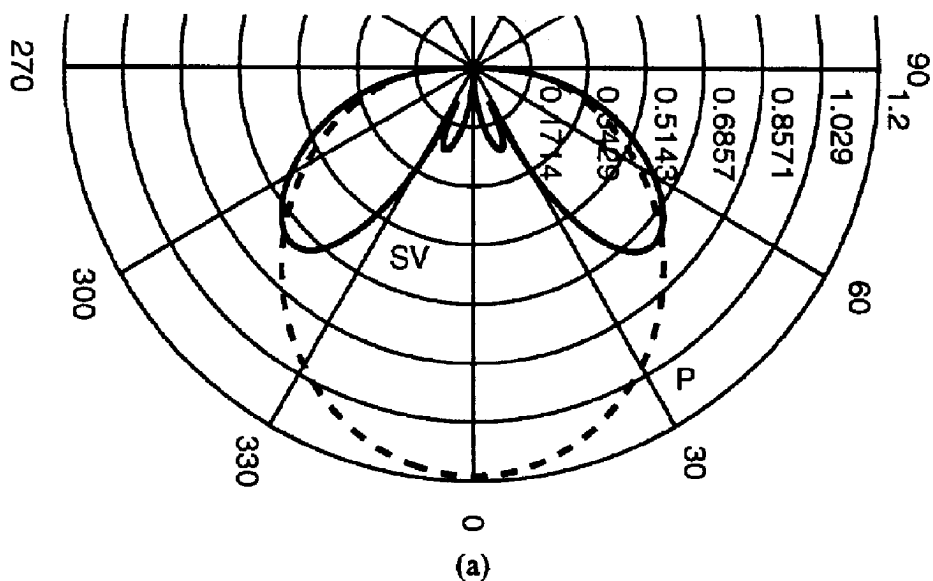
(a)
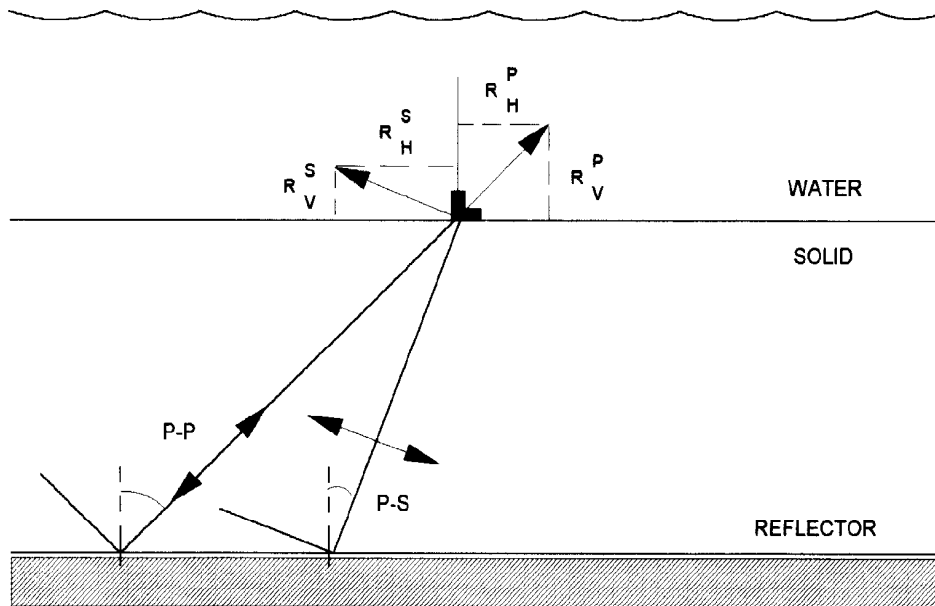
(b)

Fig. 1. (a) Schematic SUMIC (subsea seismic) 2-D acquisition (after Berg et. al., 1994).
(b) Geometry of waves impinging on a vertical and horizontal geophone at the
fluid-solid interface (after Ferber, 1989).

RESPONSE OF VERTICAL GEOPHONE
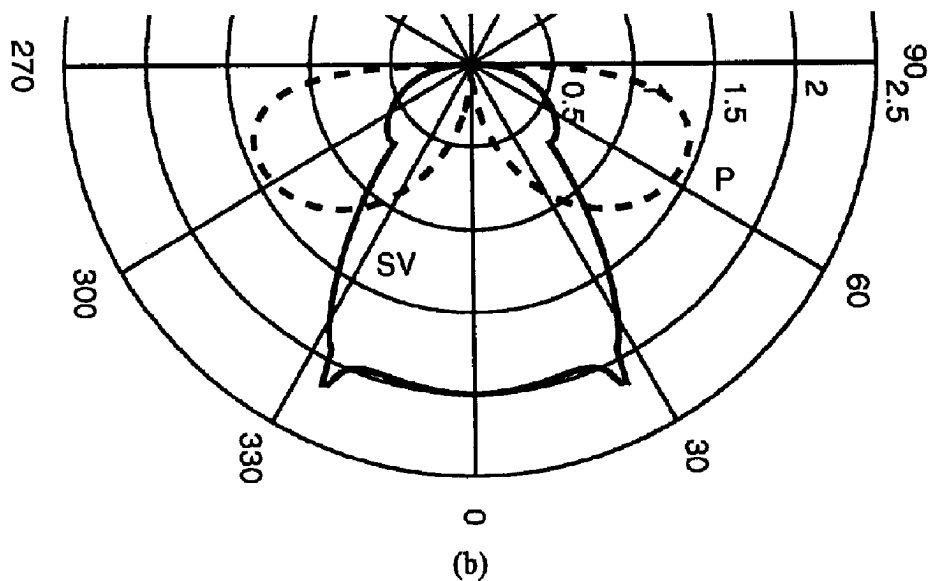

(a)

RESPONSE OF HORIZONTAL GEOPHONE

(b)

Fig 2. Response, in polar diagram form, of the vertical (a) and horizontal (b) geophones, located at a liquid-solid contact, for P waves and S waves as a function of angle of incidence. Parameter values for this case are: $Vp = 1500$ m/s, $Vs = 650$ m/s, and $\rho = 1.6$ g/cc (in the solid) and $Vp = 1455$ m/s and $\rho = 1.135$ g/cc in the liquid.

RESPONSE OF VERTICAL GEOPHONE

(a)

RESPONSE OF HORIZONTAL GEOPHONE

(b)
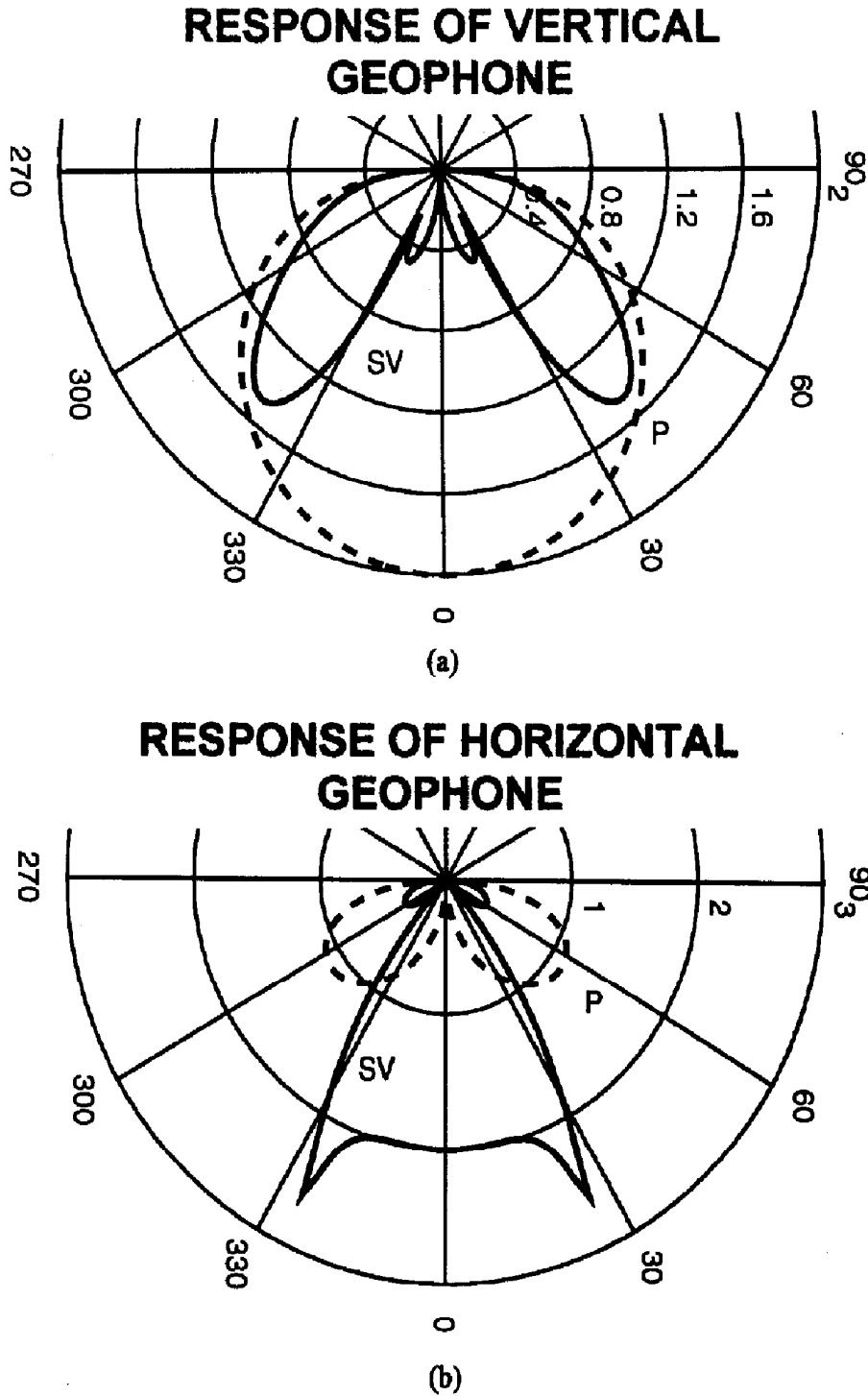
Fig. 3. Response, in polar diagram form, of the vertical (a) and horizontal (b) geophones located on the surface of a solid (stress free) for P waves and S waves as a function of angle of incidence. Parameter values are: $Vp= 1500$ m/s, $Vs= 650$ m/s, and $\rho= 1.6$ g/cc.
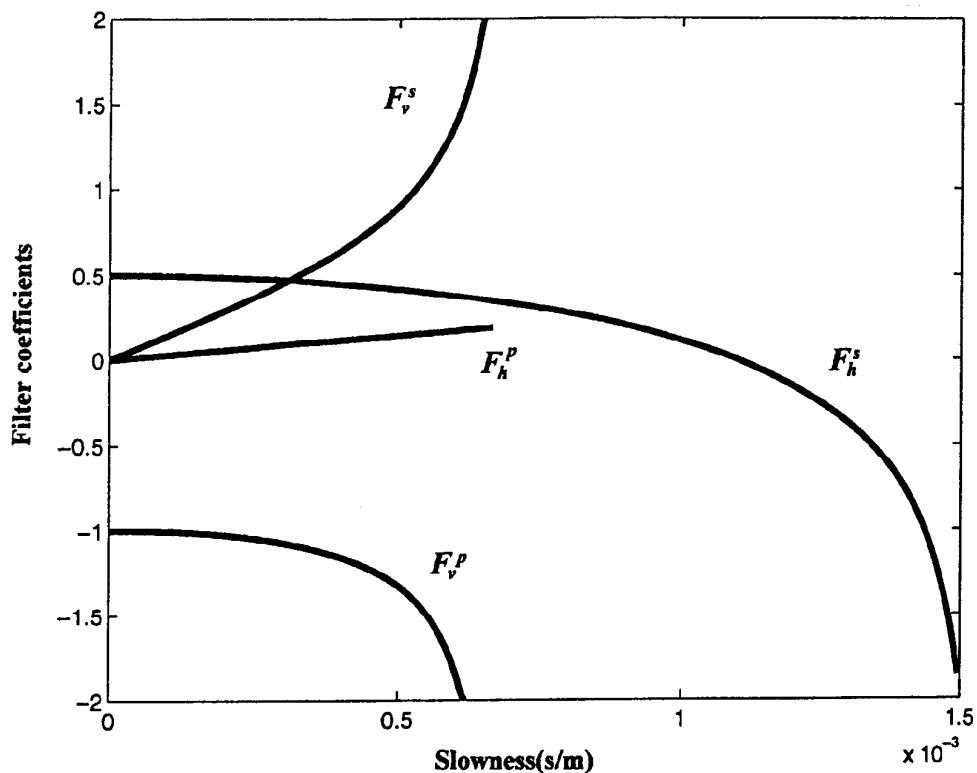
Fig. 4a. Filter coefficients F as a function of horizontal slowness for pass-P and pass-S filter for a geophone located at a liquid-solid contact as described in Fig. 2.
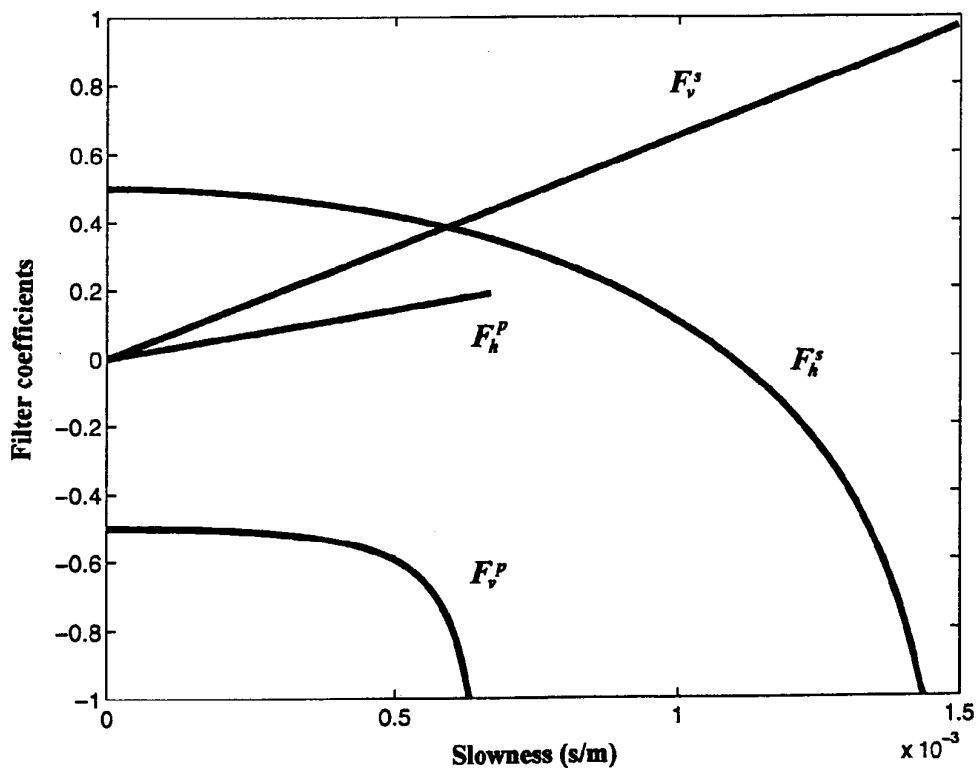

Fig. 4b. Filter coefficients F as a function of horizontal slowness for pass-P and pass-S filter for a geophone on the surface at a solid (stress-free case) using the model of Fig. 3.
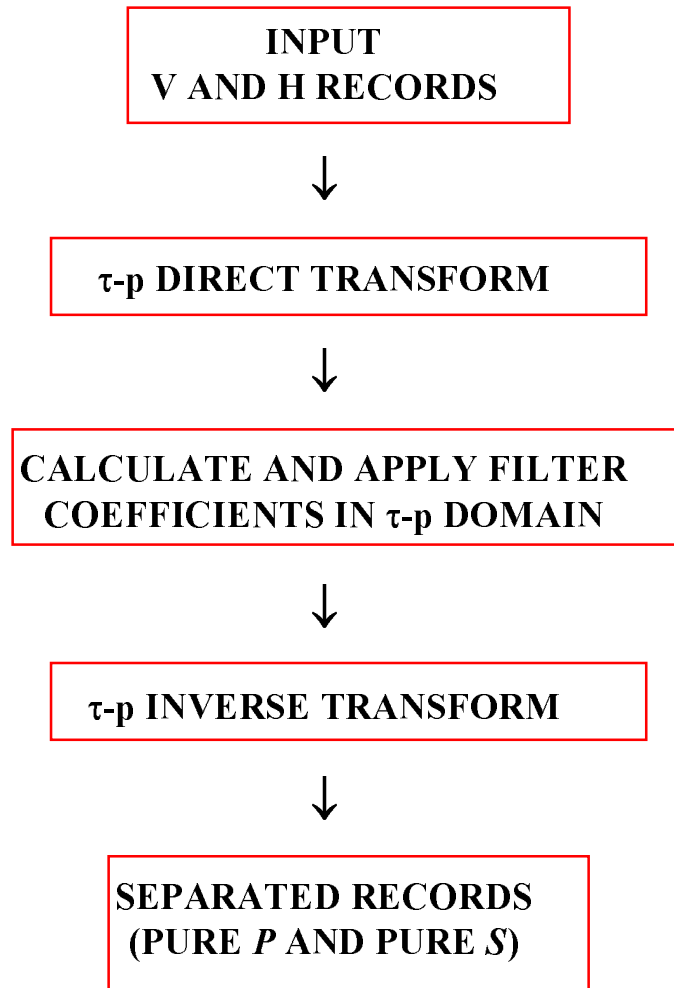
INPUT
V AND H RECORDS

↓

τ-p DIRECT TRANSFORM

↓

CALCULATE AND APPLY FILTER
COEFFICIENTS IN τ-p DOMAIN

↓

τ-p INVERSE TRANSFORM

↓

SEPARATED RECORDS
(PURE *P* AND PURE *S*)

Fig. 5. Flowchart of the P-S separation filter in the τ-p domain

HORIZONTALLY LAYERED EARTH MODEL

```
//////////////////////////////////////////////////Z= 0 m
//////// 1.135 ///////, 1455 ///, water layer///
```
10 m

ρ =1.6 g/cc   Vp=1500 m/s   Vs=650 m/s

40 m

1.7   1700   750

70 m

1.75   1900   800

110 m

1.7   1750   750

160 m

1.9   2100   950

210 m

2.0   2800   1400
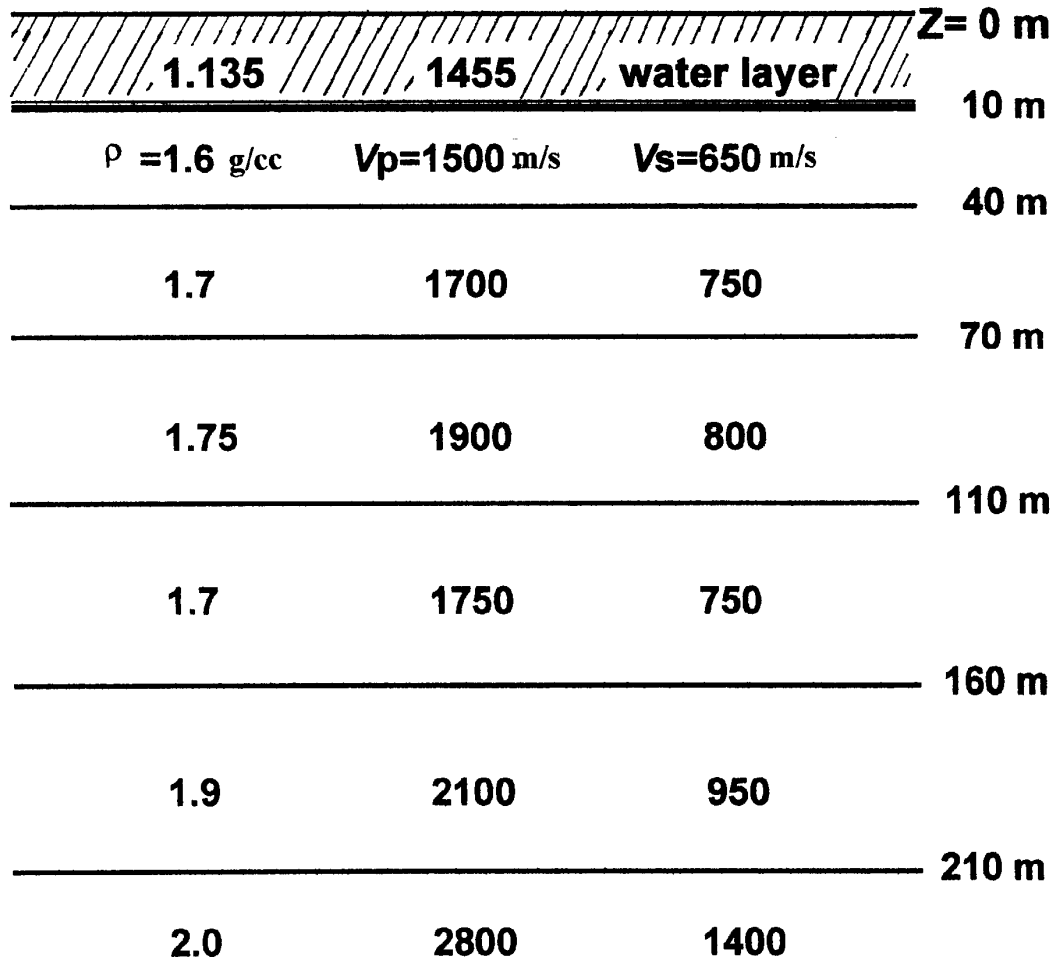
Fig. 6. Subsurface model used for synthetic data calculation (after Dankbaar, 1985).
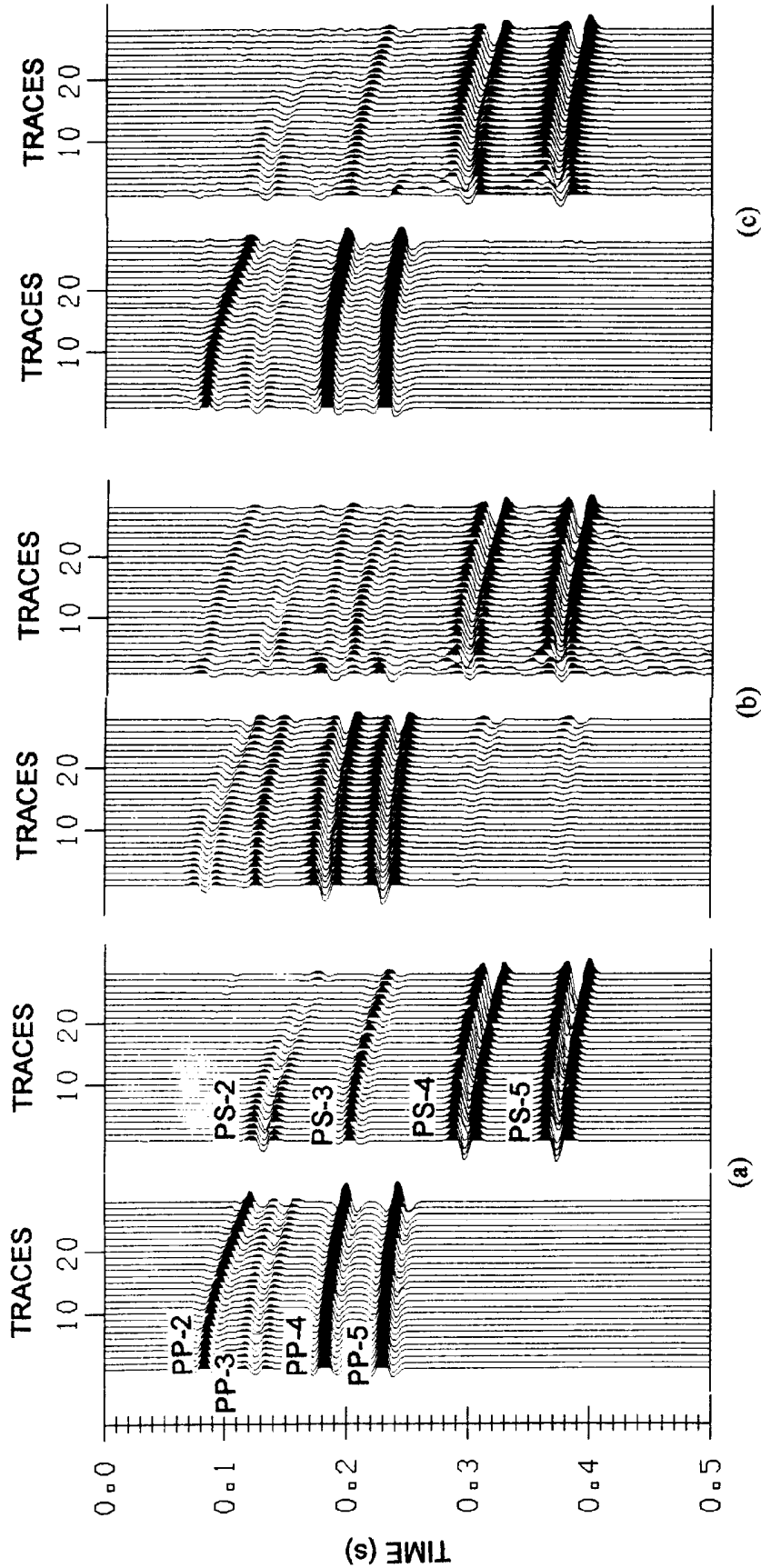
Fig. 7. Vertical and horizontal geophone response from the model of Fig. 6.
(a) *P-P* and *P-S* reflections, with no receiver response.
(b) Vertical and horizontal geophone output from incident *P-P* and *P-S* reflections.
(c) Pass-*P* and pass-*S* sections obtained from both vertical and horizontal records (Fig. 7b) using $V_p = 1500$ m/s, $V_s = 650$ m/s, and $\rho = 1.6$ g/cc (in the solid) and $V_p = 1455$ m/s and $\rho = 1.135$ g/cc (in the liquid).
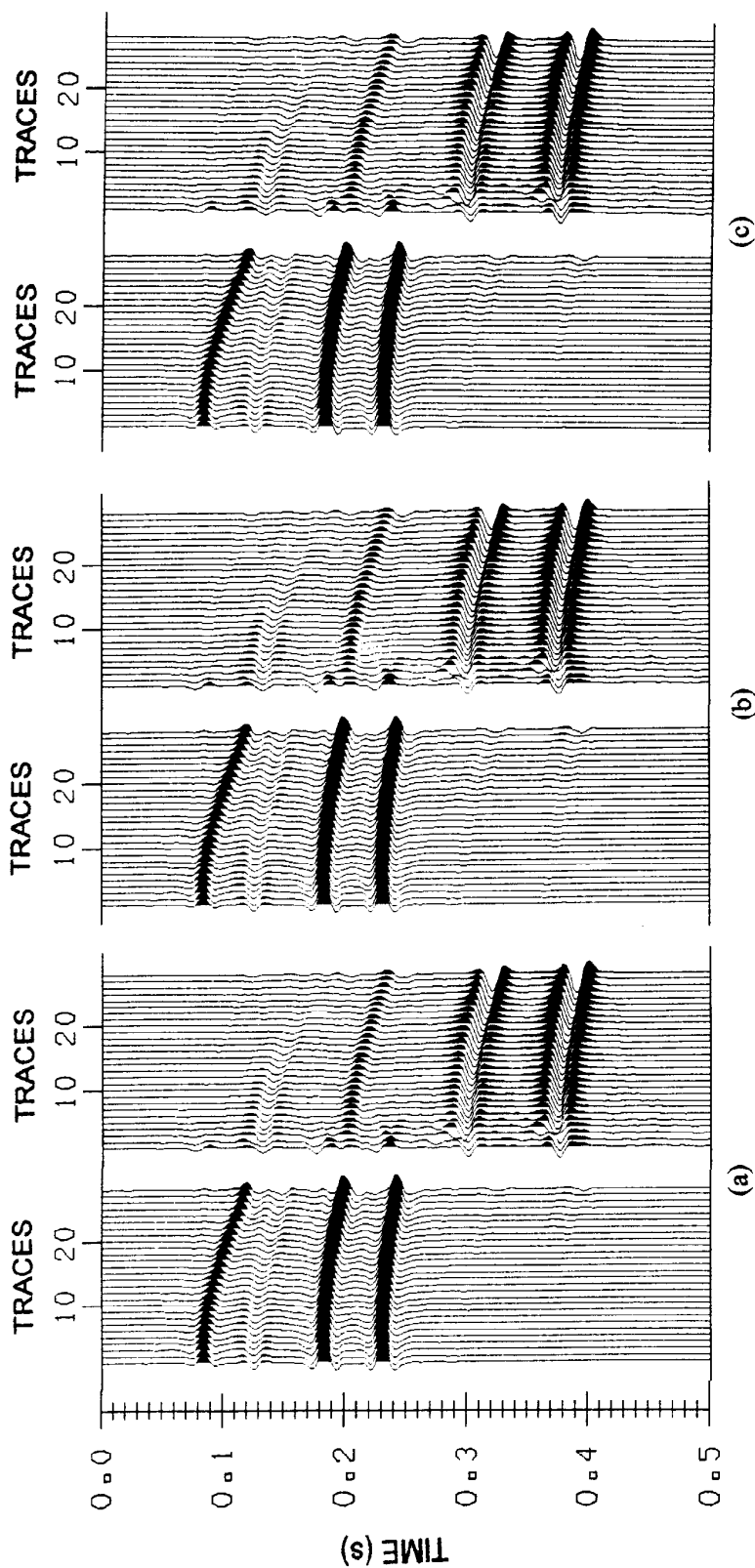
Fig. 8. a) Filtered pass-*P* and pass-*S* record, respectively, obtained using V_p= 1600 ms, V_s= 750 m/s, and ρ= 1.6 g/cc (in the solid) and V_p= 1455 m/s and ρ= 1.135 g/cc (in the liquid).
b) Filtered pass-*P* and pass-*S* record, respectively, obtained using V_p= 1700 ms, V_s= **850** m/s, and ρ= 1.6 g/cc (in the solid) and V_p= 1455 m/s and ρ= 1.135 g/cc (in the liquid).
c) Filtered pass-*P* and pass-*S* record, respectively, obtained using V_p= 1600 ms, V_s= **800** m/s, and ρ= 1.3 g/cc (in the solid) and V_p= 1350 m/s and ρ= 1.0 g/cc (in the liquid).
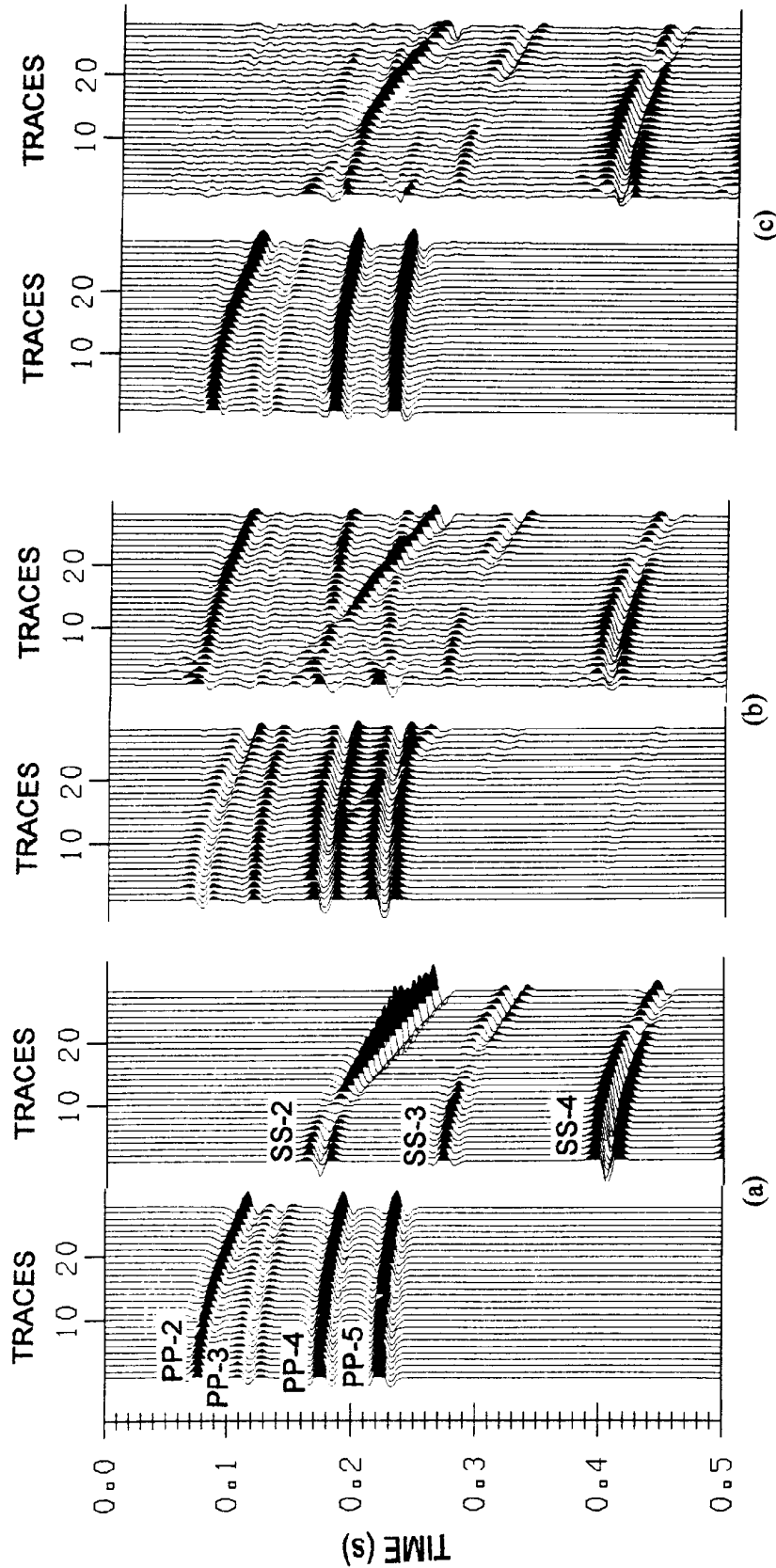
Fig. 9. Vertical and horizontal geophone response with source and receivers on the fluid-solid interface from the model of Fig. 6.
(a) *P-P* and *S-S* reflections, with no receiver response.
(b) Vertical and horizontal geophone output from incident *P-P* and *S-S* reflections.
(c) Pass-*P* and pass-*S* sections obtained from both vertical and horizontal records (Fig. 9b) using V_p= 1500 m/s, V_s= 650 m/s, and ρ= 1.6 g/cc (in the solid) and V_p= 1455 m/s and ρ= 1.135 g/cc (in the liquid).
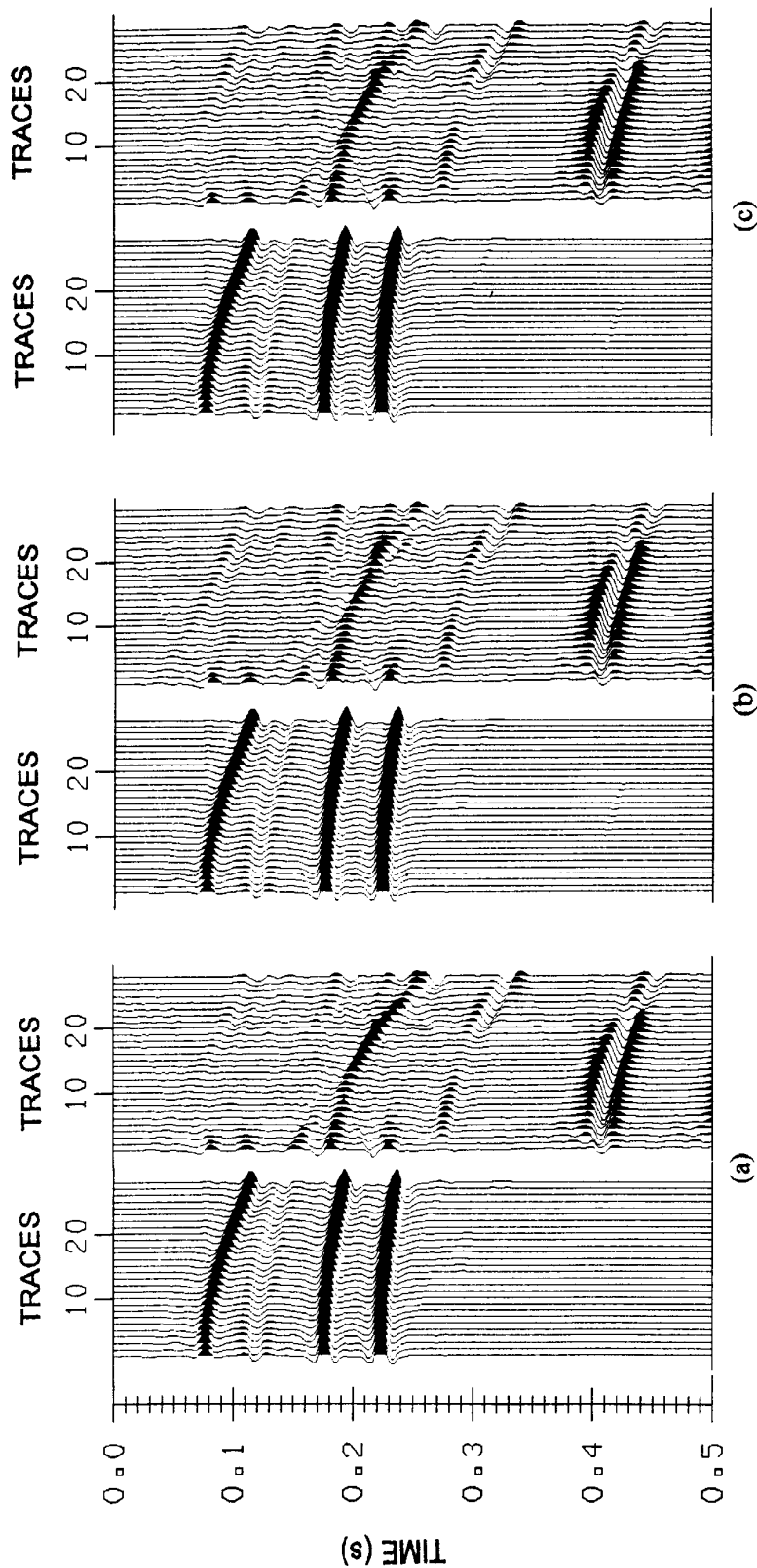
Fig. 10. a) Filtered pass-*P* and pass-*S* record, respectively, obtained using V_P= 1600 ms, V_S= 750 m/s, and ρ= 1.6 g/cc (in the solid) and V_P= 1455 m/s and ρ= 1.135 g/cc (in the liquid).
b) Filtered pass-*P* and pass-*S* record, respectively, obtained using V_P= 1700 ms, V_S= 850 m/s, and ρ= 1.6 g/cc (in the solid) and V_P= 1455 m/s and ρ= 1.135 g/cc (in the liquid).
c) Filtered pass-*P* and pass-*S* record, respectively, obtained using V_P= 1600 ms, V_S= 800 m/s, and ρ= 1.3 g/cc (in the solid) and V_P= 1350 m/s and ρ= 1.0 g/cc (in the liquid).
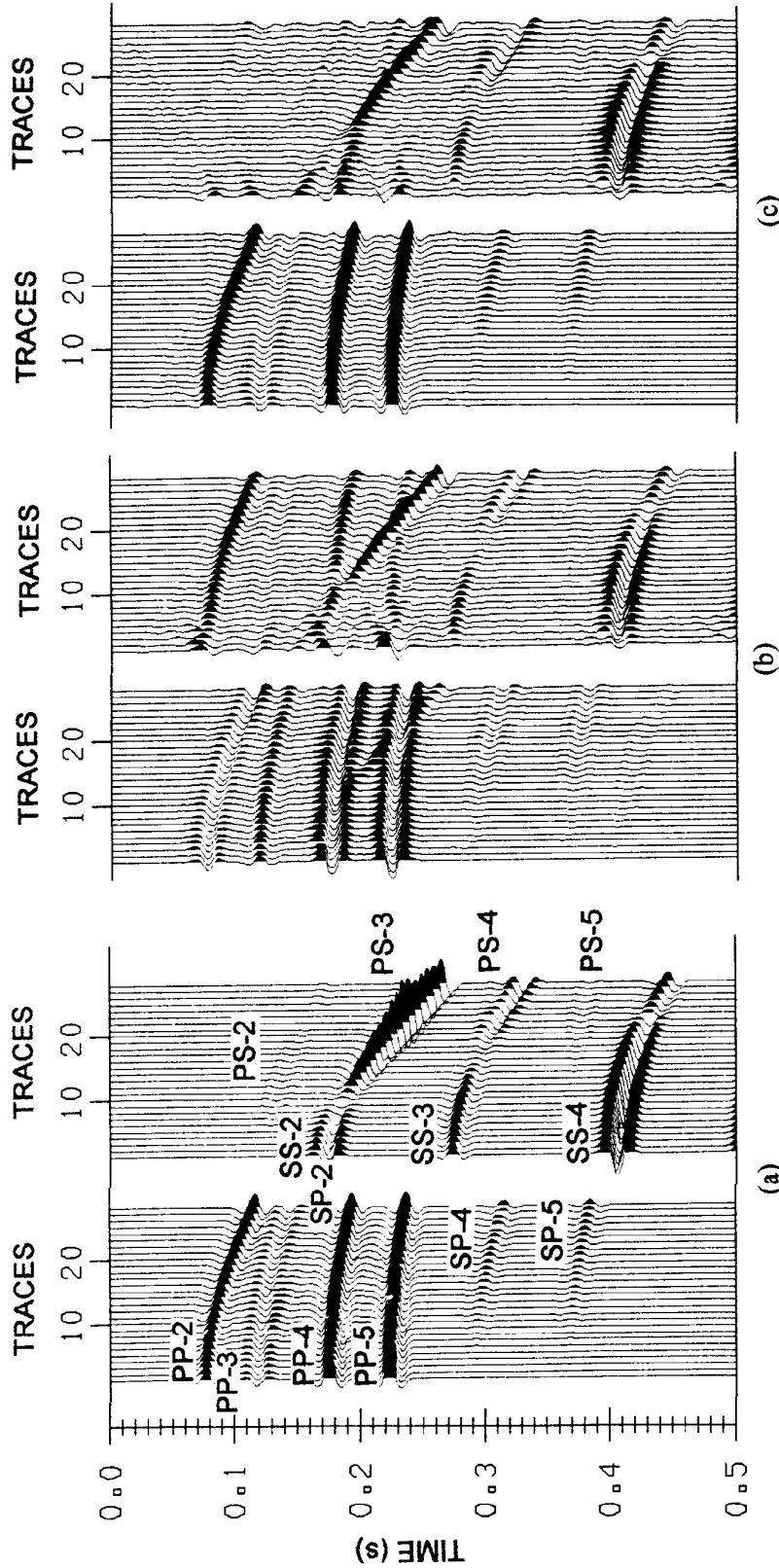
Fig. 11. Vertical and horizontal geophone response with source and receivers on the water bottom from the model of Fig. 6.
(a) *P-P*, *S-P*, *S-S* and *P-S* reflections, with no receiver response.
(b) Vertical and horizontal geophone output from incident *P-P*, *S-S*, *P-S*, and *S-P* reflections.
(c) Pass-*P* and pass-*S* sections obtained from both vertical and horizontal records (Fig. 11b) using V_p= 1500 m/s, V_s= 650 m/s, and ρ= 1.6 g/cc (in the solid) and V_p= 1455 m/s and ρ= 1.135 g/cc (in the liquid).
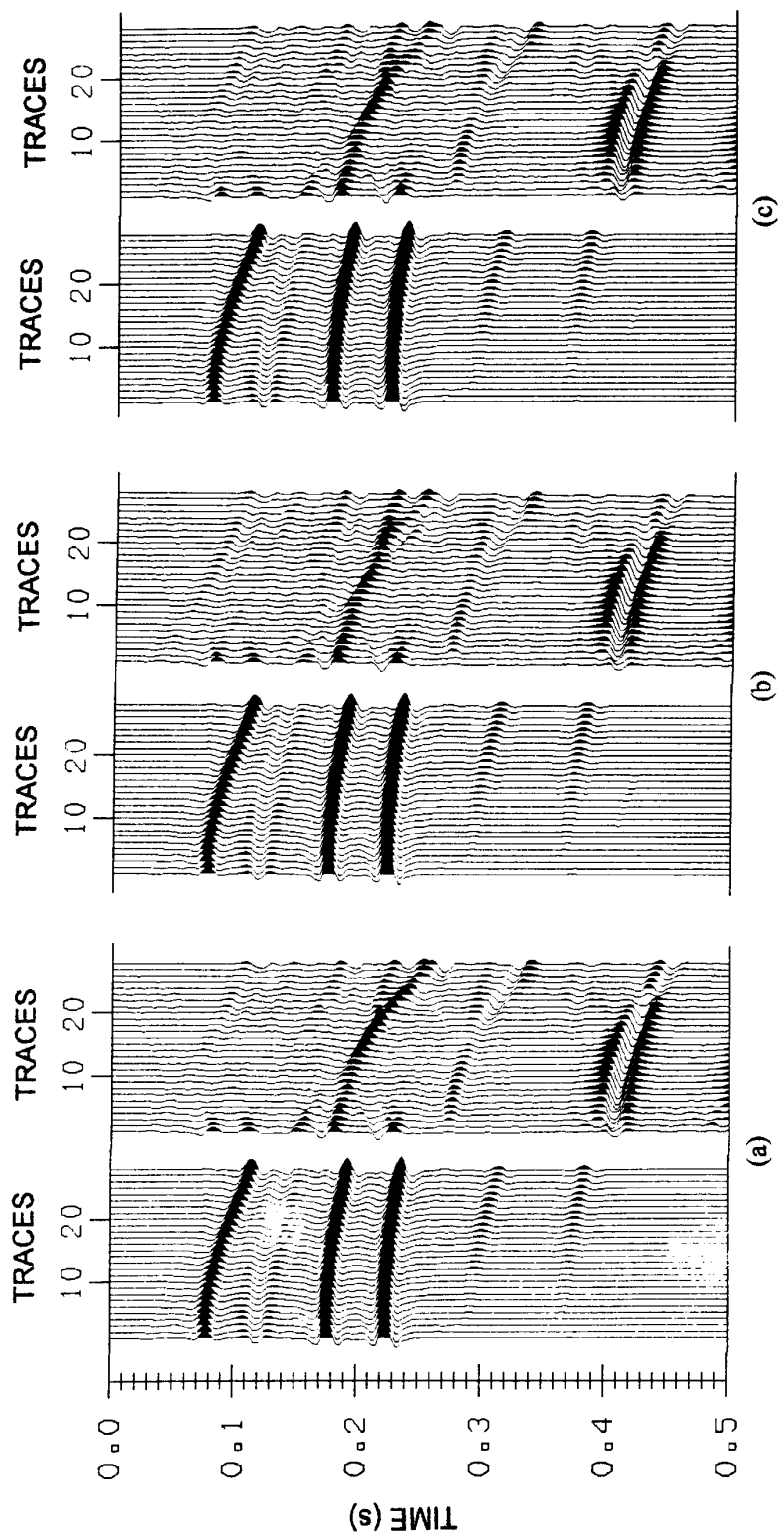
Fig. 12. a) Filtered pass-*P* and pass-*S* record, respectively, obtained using V_p= 1600 ms,
V_s= 750 m/s, and ρ= 1.6 g/cc (in the solid) and V_p= 1455 m/s and ρ= 1.135
g/cc (in the liquid).
b) Filtered pass-*P* and pass-*S* record, respectively, obtained using V_p= 1700 ms,
V_s= 850 m/s, and ρ= 1.6 g/cc (in the solid) and V_p= 1455 m/s and ρ= 1.135
g/cc (in the liquid).
c) Filtered pass-*P* and pass-*S* record, respectively, obtained using V_p= 1600 ms,
V_s= 800 m/s, and ρ= 1.3 g/cc (in the solid) and V_p= 1350 m/s and ρ= 1.0 g/cc
(in the liquid).